Journal of The Electrochemical Society, **150** (6) C440-C444 (2003)
0013-4651/2003/150(6)/C440/5/$7.00 © The Electrochemical Society, Inc.

Centrifugal Etching

An Experimental Study

R. P. Tijburg,[a] J. G. M. Ligthart,[a] H. K. Kuiken,[b] and J. J. Kelly[a,*,z]

[a]*Debye Institute, Utrecht University, 3508 TA Utrecht, The Netherlands*
[b]*Faculty of Applied Mathematics, Twente University of Technology, 7500 AE Enschede, The Netherlands*

A cell consisting of a rotatable double-walled cylinder is described for the study of etching under conditions of enhanced gravity. Rotation rates of 6000 revolutions per minute giving g values of up to 600 were possible with the set-up. The cell was tested by etching masked patterns in a copper plate with an aqueous $FeCl_3$ solution. The dependence of the etch rate on the system parameters (g value, ferric ion concentration, solution viscosity) is shown to be in agreement with trends predicted by a boundary-layer model. The results show that ''centrifugal etching'' involving artificial gravity gives a markedly increased etch rate and a reduced undercutting of the mask edge. It is shown that, in principle, the cell can be scaled up to dimensions interesting for industrial applications.
 [DOI: 10.1149/1.1573199]

Manuscript submitted July 29, 2002; revised manuscript received December 16, 2002. Available electronically April 22, 2003.

Two aspects of the wet-chemical etching of solids are generally important for practical applications. The etch rate should be as high as possible and etching should generate exactly the patterns or forms needed for the particular application. Device technology requires details with dimensions ranging from below 1 μm to above 1 cm. The maximum etch rate is achieved when the surface reactions are fast and mass transport of active etching components to the surface determines the dissolution rate. Occasionally, transport of dissolution products from the surface may be rate-limiting. With mass-transport control the etch rate depends on the diffusion coefficient of the active component (this is a system parameter) and on the steady-state concentration gradient at the surface. The latter is determined by the hydrodynamic conditions in the system.

In many applications patterns are etched through the windows in a masked substrate (Fig. 1a).[1-5] Generally, a high etch factor is desirable; this is the ratio of the etched depth d_e to the undercutting of the mask edge d_u. When the dissolution reaction is limited by mass transport, isotropic etching results. Underetching is severe (Fig. 1a) and aspect ratios close to one are obtained. The aspect ratio may be improved by jet or spray etching.[2,3,5]

Various methods can be employed to increase the etch rate in the case of mass-transport control by enhancing convective diffusion. These are based on reducing the diffusion layer thickness and thereby increasing the concentration gradient of the active component at the surface. The etching solution can be stirred either mechanically or by gas bubbling. The etching substrate can be moved with respect to the solution; the rotating-disk configuration is much used in electrochemical studies.[5-7] For large-scale industrial applications, machines are available that use jet or spray etching.[3-5]

In two earlier studies an adapted centrifuge was used to show that one can apply artificial gravity to enhance convection and increase the etch rates of both metals and semiconductors.[8,9] Since etching involves dissolution of the solid, a solution layer with a higher density is invariably formed close to the etching surface. When etching is performed in the presence of an acceleration field, for example, in a centrifuge, the more dense solution is effectively expelled from the hole if the acceleration vector is pointing out of the hole. This creates a natural convection pattern inside the hole (Fig. 1b). In this case the fresh etchant should first encounter the base of the cavity, creating the largest etch rate where it is needed. The depleted etchant passes out of the hole along the walls, ensuring a lower dissolution rate at the walls. This should give rise to an improved etch factor. Experiments carried out on bronze confirmed this effect.[8] In centrifugal etching the formation of vortices within the etching cavity at larger etch depths is avoided.[9] Such vortices, which are inherent in methods in which the etchant is forced along the hole pattern, may lead to a drastic reduction in etch rate at longer etching times and to strong undercutting of the resist.

Shin and Economou[10] used a finite element approach for the numerical modeling of centrifugal etching. By considering the shape evolution in an etching cavity partly covered by a mask, they showed that the etch factor could be greater than unity. One of us[11] has developed a boundary-layer model for free convection in the centrifugal etching of an axisymmetric cavity. This model reproduces the etched shapes predicted by Shin and Economou.[10] In addition, it yields an analytical expression relating the etch rate to the system parameters: centrifugal acceleration, concentration and the diffusion coefficient of the active etching component, solution viscosity, and etching time.

In this paper we describe an experimental study of centrifugal etching. In contrast to previous work involving an improvised etching setup,[8,9] we have designed a simple and versatile cell. This prototype was tested with an etching system, copper in aqueous $FeCl_3$ solution, widely used in technological applications.[1-3] Etching does not involve gas evolution which would be a complicating factor. We compare our results with those expected from the boundary-layer model[10] and consider the possibility of scaling up the system.

Experimental

The cell design.—The cell was designed so that it could be easily taken apart in order to mount and demount the substrate. The principle of the design is shown schematically in Fig. 2. The cell consists of two concentric cylinders, an inner cylinder I, and an outer cylinder O. The etchant (the shaded area) is contained in the open space between the two cylinders. The substrate S to be etched is mounted on the outer wall of the inner cylinder. A cap, which is not shown, prevents the etchant from escaping during operation. The cell is rotated about its axis, giving rise to an acceleration field at the surface of the etching substrate. The bulk of the solution is stationary with respect to the rotating walls during etching.

The detailed design is shown in Fig. 3. Figure 3a gives an exploded view of the cell parts, which were made from Perspex; Fig. 3b-d show sections through the parts. The cell is assembled from three main parts: an outer hollow cylinder 1, an inner hollow cylinder with two flattened sides 5 (this is the sample holder) and a solid spacer 3 to position the inner and outer cylinders with respect to each other. The outer cylinder 1 has a wide top and a narrow base with a screw thread on the inner surface of the base. An O-ring 2 fits into a concentric groove in the base of the wide part of cylinder 1. The solid spacer 3 has a threaded base which can be screwed into the bottom part of cylinder 1. In this way the spacer is pressed tightly against the O-ring 2 in the base of the cylinder, ensuring a leak-free seal at the bottom of the cell. The sample holder 5 fits snugly over the top part of the spacer, thus creating a compartment

* Electrochemical Society Active Member.
z E-mail: J.J.Kelly@phys.uu.nl

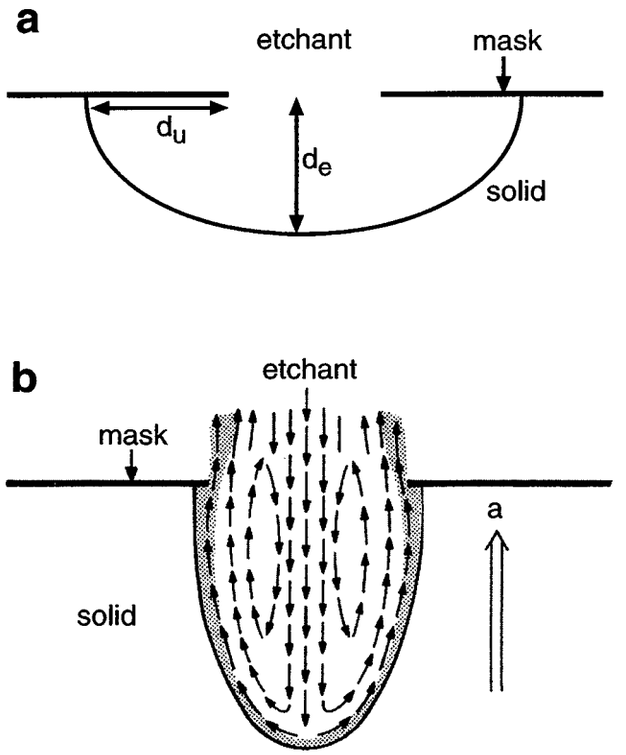

Figure 1. (a) A schematic profile of a cavity obtained by isotropic etching of a solid through a window in a mask. The etch factor is defined as the ratio of the etched depth d_e to the undercutting of the masked edge d_u. (b) Schematic of the effect of an acceleration field "a" on mass transport for etching of the cavity. Arrows denote the direction of flow of the etchant. Reaction products occupy the dotted region.

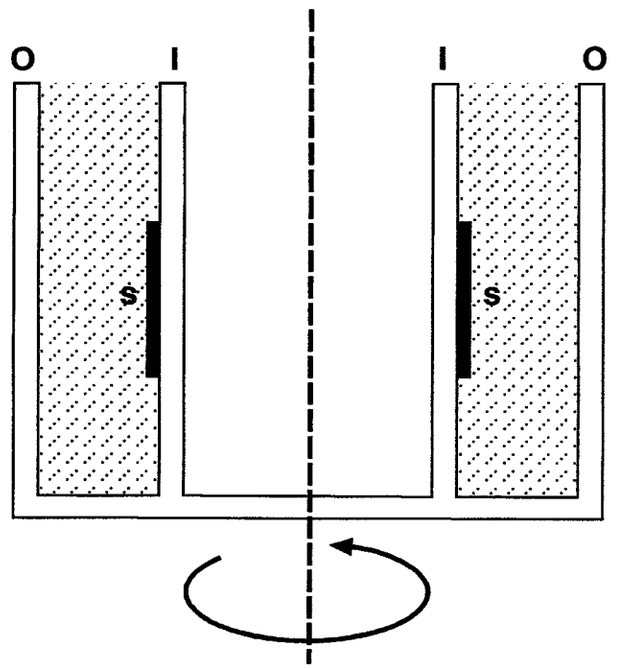

Figure 2. The basis for the design of the centrifugal etching cell. See text for details.

for the etchant between the inner and outer cylinders (see also Fig. 2). The sample holder and spacer are locked by two pins 4 which fit into holes in each piece. The sample holder has two flattened sides with grooves (see Fig. 3a) into which the copper plate samples could be easily mounted. The normal distance from the center of the cell to the exposed copper surface is 15 mm. The cell is sealed at the top with an O-ring 6 and a lid 7 which is screwed into the outer cylinder. A hole in the lid allows excess etchant to escape from the cell during loading.

The cell was mounted on bearings and rotated about its axis with a belt fitted to the lower part of cylinder 1 and a motor with a control unit and a feedback system. Rotation rates up to 6000 rpm (corresponding to g values up to 600) were possible with the setup. The rotation rate was checked with a stroboscope.

The etching system.—As a model system we studied the dissolution of copper in aqueous $FeCl_3$ solution. Etching in this case is determined by mass transport of ferric ions to the surface. An aqueous stock solution containing 3.7 mol/L $FeCl_3$ with 7 vol % concentrated HCl was used either as prepared or diluted to give a range of etchants of different ferric ion concentrations and viscosity. The viscosity of the etchants was determined by the Ubbelohde method and the results agreed with those previously reported for $FeCl_3$ solutions.[12]

The copper plate was masked with resist by standard photolithographic techniques. The masked pattern contained circular windows with diameters ranging from 10 to 1000 μm. Before etching, the copper was pretreated for 10 min in a solution containing 3 g of ethylenediamine tetra-acetic acid in 100 mL of water, acidified with three drops of concentrated HCl. The etched depth and hole broadening due to undercutting were determined by optical microscopy after removal of the resist layer. Cross sections of etched holes were also made and studied by microscopy.

Results

The etch rate, defined as the depth etched per unit time, was studied as a function of the solution composition and the rotation rate of the cell at room temperature (20 ± 1°C). In all the experiments reported here two etching times were used, 5 and 10 min. Within the accuracy of the measurements the etch rate was essentially constant in this range. Some experiments were performed at an etching time of 20 min; the total etch rate in this case was somewhat lower than that for the shorter term experiments. From Fig. 4a, which shows results for a 100 and 200 μm hole etched with a 2.5 mol/L $FeCl_3$ solution, it is clear that the etch rate increases markedly with increasing g value. At 600 g the etch rate is a factor of 15 higher than that measured without rotation (2 μm/min). Figure 4b gives the etch factor as a function of g value for the experiment of Fig. 4a. Ratios of above four were found, confirming that centrifugal etching can indeed reduce the effect of undercutting of the mask. The surface of the copper after etching was smooth and showed Bénard-cell formation, similar to that reported previously for bronze.[8]

The plot of etch rate *vs.* $FeCl_3$ concentration (Fig. 5) exhibits a maximum at around 2 mol/L. This result is typical for all the etching combinations (hole diameter and g values) that we have investigated. The influence of the dimensions of the hole on the enhancement of the etch rate is shown in Fig. 6 for a 2.5 mol/L $FeCl_3$ solution. The etch rate is plotted as a function of hole diameter (on a logarithmic scale) for various g values. While a marked increase in the etch rate is observed during cell rotation for holes with a diameter of 100 and 200 μm (see also Fig. 4), we observe a slight decrease in etch rate for larger holes. On the other hand, the effect of enhanced gravity on small holes (diameter ≤50 μm) is much less pronounced; this holds for g values up to 600.

Discussion

Before considering our results, we briefly review the analytical model[11] that has been developed to describe etching of an axisym-

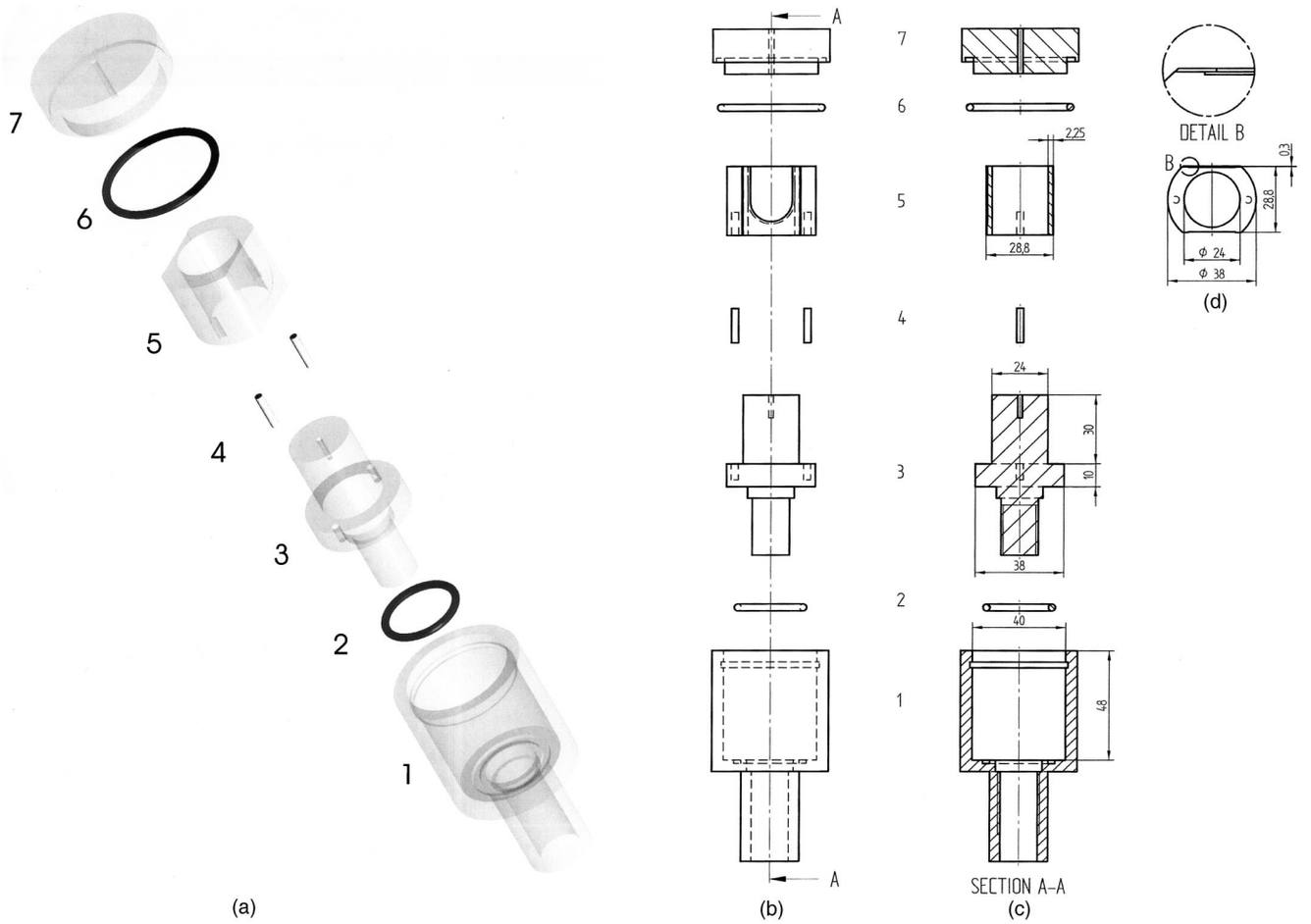

Figure 3. The detailed cell design: (a) an exploded view of the cell parts, (b-d) sections through the parts. The dimensions are in millimeters. See text for details.

metric cavity under the influence of an artificial acceleration field. The etching process is governed by a thin convective-diffusive boundary layer along the curved cavity wall. The boundary-layer model can be solved explicitly to give an exact representation of mass transport at the wall. The solution is substituted in the moving-boundary condition; this results in an expression for the wall position as a function of time. This equation can be used to obtain a one-parameter family of similarity curves, *i.e.*, cavity shapes, such as those shown in Fig. 7a. The shape of the cavity, which is time independent, is determined by a free parameter α, which can be fixed only on the basis of the initial geometry of the etching system. The lowest value with physical significance ($\alpha = 0.7566$) gives a bulging profile with an almost flat bottom (case a, Fig. 7a). A profile for $\alpha = 1$ (case b, Fig. 7a) is quite similar to the long-time profile calculated by Shin and Economou.[9] When α is further increased (up to 3 in Fig. 7a) the profile becomes pear-shaped and elongated. Figure 7b shows a typical cross section through an etched hole in a copper plate. The agreement between this characteristic profile and that predicted by theory (see Fig. 7a) supports the validity of the model; the measured profile corresponds to an α value of about 1.5.

Equation 65 of Ref. 11 gives an expression for the centrifugal etch rate v_n as a function of the system parameters for a family of similarity shapes. If we restrict ourselves to the center of the etched pit, then the right side of that equation will reduce to some numerical constant and we have

$$v_n \sim \gamma t^{-1/5} \qquad [1]$$

where t is the time and γ is given by (see Eq. 1, 36, and 40 of Ref. 11)

$$\gamma \sim (\sigma_e c_m)^{4/5} \left(\frac{aBc_m}{\nu D} \right)^{1/5} \qquad [2]$$

Here we have disregarded some numerical constants. The notation has been modified slightly from that used in Ref. 11. In Eq. 2 a is the centrifugal acceleration (m/s^2), c_m is the maximum concentration of the active etching component (kmol/m^3), ν is the kinematic viscosity of the etchant (m^2/s), D is the diffusion coefficient of the active etching component (m^2/s), and B is a parameter (m^3/kmol) indicating how the density ρ varies with the concentration c. The latter is defined by

$$\rho = \rho_0\{1 + Bc\} \qquad [3]$$

where ρ_0 is the density at $c_m = 0$. The "etching parameter" σ_e is defined by Eq. 9 of Ref. 13 and 14 in terms of some basic physical parameters

$$\sigma_e = \frac{DM_s}{m\rho_s} \qquad [4]$$

where M_s is the molecular weight of the solid (kg/kmol), ρ_s is its density (kg/m^3), and m represents the number of moles of active etching component required to dissolve *1 m* of the solid.

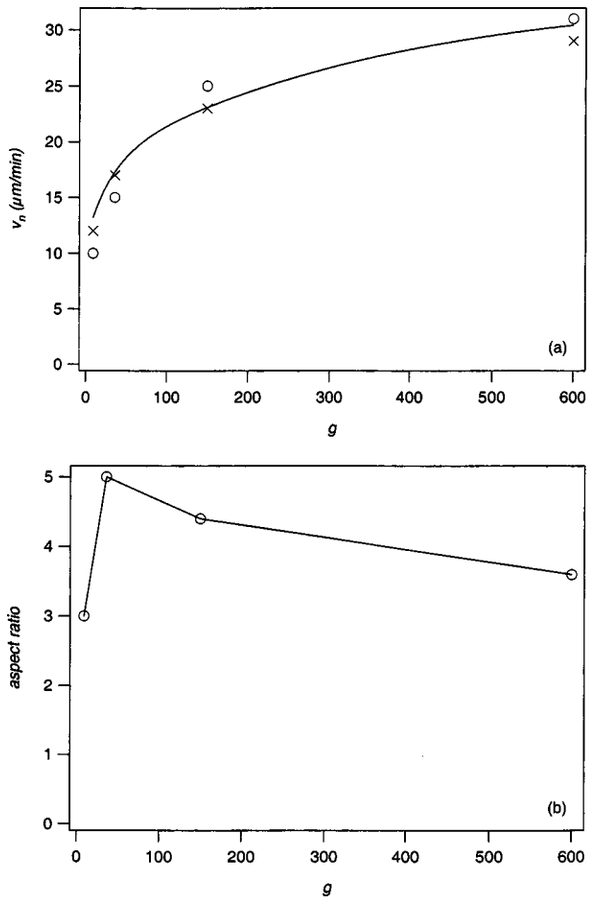

Figure 4. (a) The dependence of etch rate on the g value for the etching of (○) 100 and (x) 200 μm holes using a 2.5 mol/L $FeCl_3$ solution; (——) shows a $g^{1/5}$ dependence. (b) Dependence of etch factor on the g value for 100 μm holes.

Apart from a constant proportionality factor, the etch rate v_n can now be expressed explicitly in terms of the system parameters

$$v_n \sim \left(\frac{M_s}{m\rho_s}\right)^{4/5} c_m D^{3/5} \nu^{-1/5} (aB)^{1/5} t^{-1/5} \qquad [5]$$

The model predicts a slow decrease in etch rate with time (a $t^{-1/5}$ dependence). The time domain of most of our measurements is too limited to allow us to check this dependence. We do, however, see a drop in etch rate at longer etching times. From Eq. 5 it is clear that the etch rate should be mainly determined by four parameters: the acceleration field, the concentration of oxidizing agent, the viscosity, and the diffusion coefficient. The latter two parameters depend on the $FeCl_3$ concentration. Log-log plots of the etch rate *vs.* accelera-

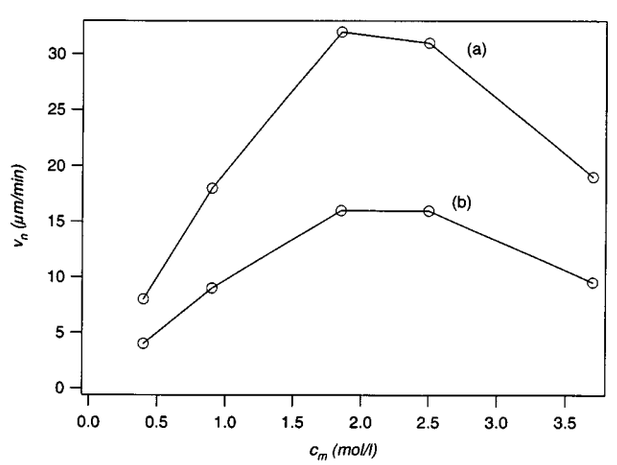

Figure 5. A plot of the etch rate *vs.* $FeCl_3$ concentration for a 100 μm hole at two different g values: (a) 600 and (b) 36.

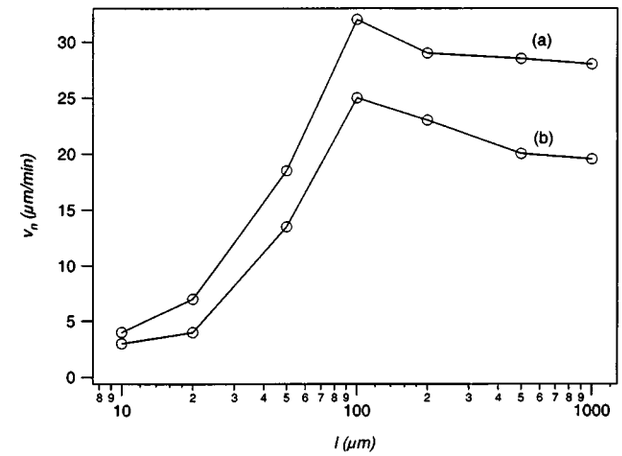

Figure 6. The dependence of etch rate on the hole diameter (l) for a 2.5 mol/L $FeCl_3$ etchant at two different g values: (a) 600 and (b) 150.

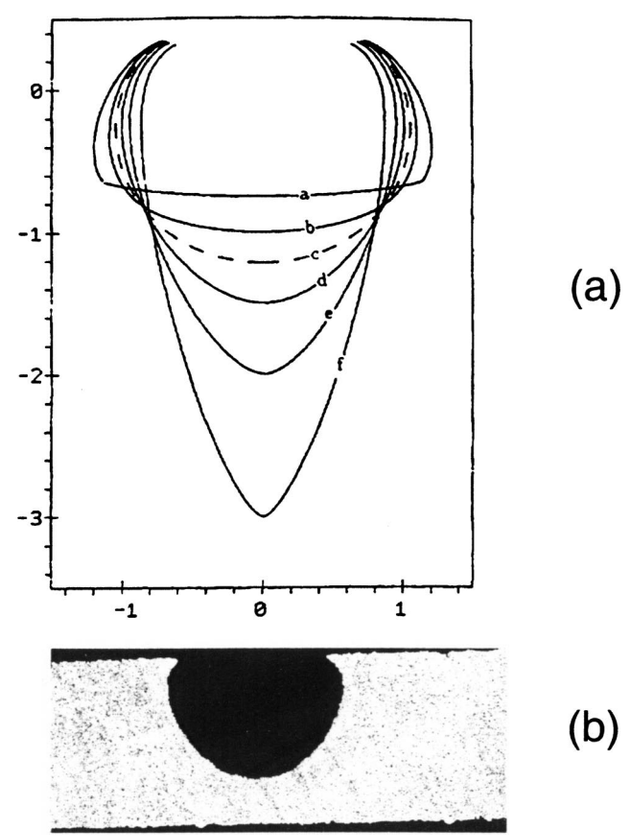

Figure 7. (a) Selection of similarity curves calculated from the model.[11] The horizontal and vertical coordinates have been scaled by the same factor. The free parameter α has values (a) 0.7566, (b) 1, (c) $(8/3)^{1/5} = 1.21673$, (d) 1.5, (e) 2, and (f) 3. (b) Cross section through an etched hole.

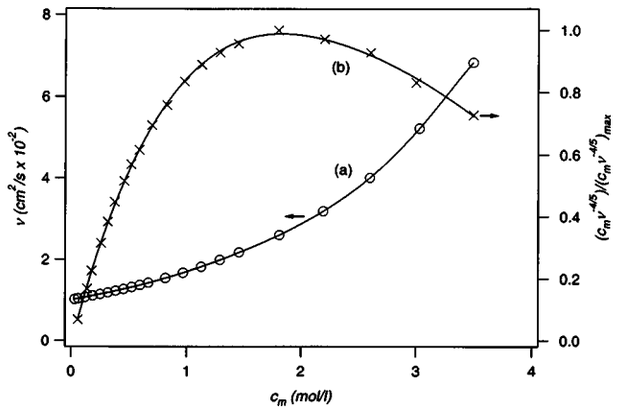

Figure 8. Dependence of (a) ν and (b) $c_m \nu^{-4/5}$ on the Fe Cl_3 concentration at 20°C (data from Ref. 12, see Eq. 7). $c_m \nu^{-4/5}$ is normalized with respect to the value at the maximum.

tion field give straight lines with slopes varying between 0.2 and 0.25, close to the exponent predicted by theory (Eq. 5). The $a^{1/5}$ dependence, shown as a solid line in Fig. 4a, fits the results quite well, except at low rotation rates.

The rather unusual concentration dependence of the etch rate (Fig. 5) can be understood by realizing that as the $FeCl_3$ concentration increases, the viscosity increases, and consequently, the diffusion coefficient decreases. An accurate analysis of our results in terms of Eq. 5 is not possible. For concentrated solutions, such as those used in the present work, activity should be used instead of concentration. We do not have data for the activity coefficients and diffusion coefficients of the Fe^{3+} ion in our system. However, the general trend in etch rate as a function of concentration can be demonstrated. Easteal *et al.*[15] measured the viscosity and diffusion coefficient of $FeCl_3$ solutions, acidified with HCl at 25°C. From their results we find the diffusion coefficient to be inversely proportional to the kinematic viscosity

$$\nu D = \nu_o D_o \qquad [6]$$

where ν_o is the viscosity for $c_m = 0$ and $D \rightarrow D_o$ as $c_m \rightarrow 0$. Inserting Eq. 6 into Eq. 5 for the etch rate we obtain

$$v_n = A c_m \nu^{-4/5} \qquad [7]$$

where A includes the variables a and t. If we assume that a relation similar to Eq. 7 also holds for our system at 20°C and to higher concentrations, then we can use the available values of ν (curve a of Fig. 8[12]) to calculate $c_m \nu^{-4/5}$ as a function of c_m. The corresponding plot, given as curve b in Fig. 8, shows a maximum similar to that of the measured etch rate as a function of c_m (Fig. 5).

The acceleration field obviously has a much weaker influence on the etching of smaller holes (diameter <50 μm). According to the model[11] a significant enhancement of the etch rate is expected only if the Rayleigh number Ra is much larger than unity

$$\mathrm{Ra} = \frac{a \beta \Delta c l^3}{\nu D} \gg 1 \qquad [8]$$

The parameters a, B, ν, and D have already been introduced in relation to Eq. 2; $B\Delta c$ is the relative density increase where Δc is the maximum concentration difference. Further, l is a length parameter characteristic of the size of the cavity, *e.g.*, the dimensions of the mask opening, which in the present case corresponds to the hole diameter. For small holes the requirement of Eq. 8 is not met. This equation indicates that etch-rate enhancement for small dimensions can be achieved either by increasing the centrifugal acceleration and the relative density increase or by decreasing viscosity and diffusion coefficient; the latter depends on the etchant choice.

The most significant increase in etch rate and the improvement in aspect ratio are observed at lower g values (see Fig. 4a and b). This means that the cell can be operated effectively at moderate rotation rates and consequently, can be scaled up to give an industrial etching machine. In addition, since the centrifugal force is proportional to $\omega^2 r$, where ω is the radial velocity and r the effective radius, the rotation rate required to maintain a given g value decreases as the radius of the cylinder increases. If the effective radius of the cell is increased by a factor of 10 (from 1.5 to 15 cm), then the rotation rate needed to achieve a g value of 150 is 950 rpm. This should be easy to realize, as experience with commercial washing machines shows. For larger etching machines a horizontally rotating cylinder may be more practical than the setup with vertical rotation used for laboratory experiments in the present study. Centrifugal etching machines would be particularly interesting for etching foils; in this case the foil can be rolled onto the outer surface of the inner cylinder.

The cell described here can be easily adapted for experiments with the acceleration field vector pointing in the opposite direction.[8] In this case the substrate should be mounted on the inner surface of a demountable outer cylinder.

Recently, Atobe *et al.*[16] used an adapted centrifuge to investigate the electro-oxidative polymerization of aniline. Lin and Navarro used a similar setup to study metal electrodeposition.[17] The cell described in the present work would also be suitable for studying the influence of centrifugal force in such electrochemical systems. A reference and a counter electrode could be mounted together with the substrate (the working electrode) in the solution compartment of the present cell. With electrical leads passing from the electrodes through the wall of the inner cylinder to brush contacts on the inner surface, electrochemical parameters could be measured as a function of the g value.

Acknowledgments

We thank Ing. Johan van der Linden for designing and building the control unit and Dr. Marcel de Bruyn for providing the photolithographic facilities and for his help with the project. This work was made possible by funding from the Netherlands Foundation for Technical Research (STW, project no. TW44.3286).

Utrecht University assisted in meeting the publication costs of this article.

References

1. *Thin Film Processes*, J. L. Vossen and W. Kern, Editors, Academic Press, New York (1978).
2. L. T. Romankiw, in *Etching for Pattern Definition*, H. G. Hughes and M. R. Rand, Editors, PV 76-3, p. 161, The Electrochemical Society Proceedings Series, Princeton, NJ (1976).
3. G. Goossen and J. van Ruler, Proceedings of the World Conference on Metal Finishing, Interfinish, Amsterdam (1976).
4. D. M. Allen, *The Principles and Practice of Photochemical Machining and Photoetching*, Hilger, Bristol (UK) (1986).
5. R. Ueda, S. Toki, Y. Tanozaki, and T. Sugiutra, *Met. Finish.*, **1994**, 29.
6. H. K. Kuiken, E. P. A. M. Bakkers, H. Ligthart, and J. J. Kelly, *J. Electrochem. Soc.*, **147**, 1110 (2000).
7. O. Piotrowski, C. Madore, and D. Landolt, *J. Electrochem. Soc.*, **145**, 2362 (1998).
8. H. K. Kuiken and R. P. Tijburg, *J. Electrochem. Soc.*, **130**, 1722 (1983).
9. L. N. Vozmilova and N. V. Glazunova, *Izv. Akad. Nauk SSSR, Neorg. Mater.*, **23**, 680 (1987); *Inorg. Mater. (Transl. of Neorg. Mater.)*, **23**, 606 (1987).
10. C. B. Shin and D. J. Economou, *J. Electrochem. Soc.*, **138**, 527 (1991).
11. H. K. Kuiken, *J. Eng. Math.*, **34**, 181 (1998).
12. *CRC Handbook of Chemistry and Physics*, R. C. Weast, Editor, CRC Press, Boca Raton, FL, (1987).
13. H. K. Kuiken, J. J. Kelly, and P. H. L. Notten, *J. Electrochem. Soc.*, **133**, 1217 (1986).
14. P. H. L. Notten, J. J. Kelly, and H. K. Kuiken, *J. Electrochem. Soc.*, **133**, 1226 (1986).
15. A. J. Easteal, R. Malhotra, W. E. Price, and L. A. Woolf, *J. Solution Chem.*, **20**, 319 (1991).
16. M. Atobe, S. Hitose, and T. Nonaka, *Electrochem. Commun.*, **1**, 278 (1999).
17. S. W. Lin and R. M. F. Navarro, *J. Electrochem. Soc.*, **148**, C284 (2001).